Elliptic Anisotropy from Quantum Diffraction

Erik Carrió

with Daniel Pablos arXiv:2603.12346, Phys.Rev.D 114 (2026) 1, 014015

and Xoán Mayo López WIP

EMMI Workshop: Probing the early stages with jets
13th. July 2026

Universidad de Oviedo
ICTEA

Smashing Large Ions

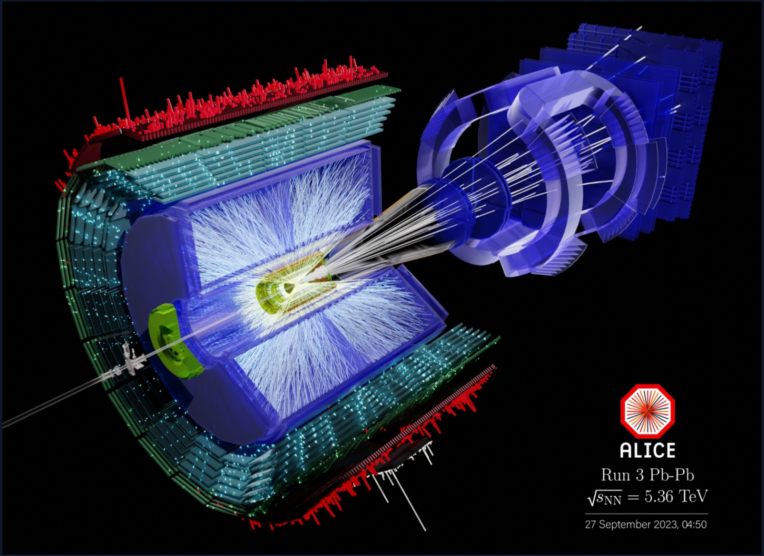

Preferred Orientations

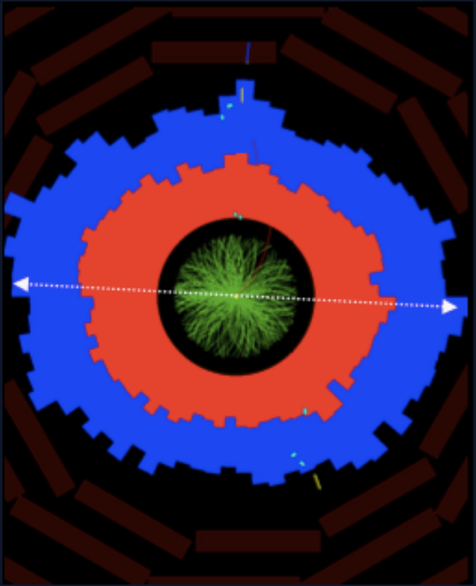

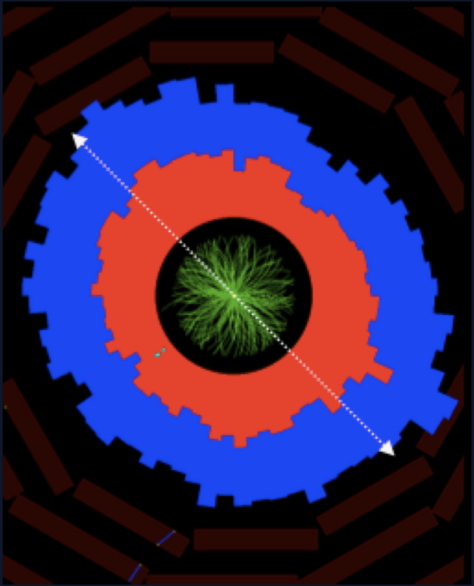

Collective Explosion

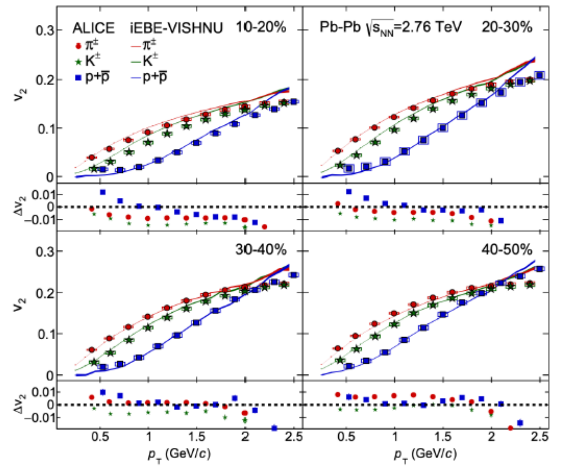

ALICE - 1606.06057

- Initial geometric anisotropy
- Anisotropic pressure gradients
- Final anisotropy in momenta

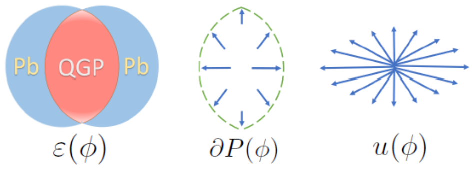

Azimuthal Anisotropy due to Energy Loss

- Energetic particles (jets) are produced in the initial hard collision.
- As they escape, they interact with the dense background medium.
- Particles traveling along the long axis lose significantly more energy.
- This **selection bias** means the surviving high-energy particles tend to align with the short axis.

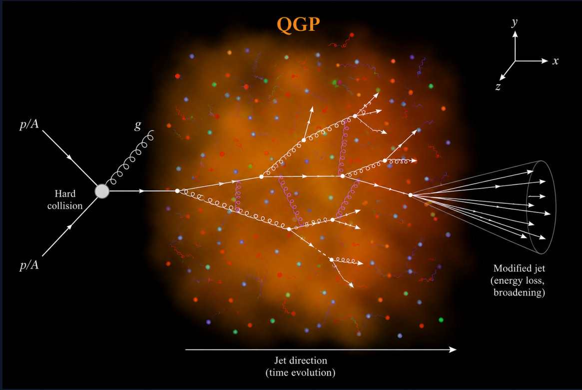

See J. Bahder's talk today for drift effects on v_2.

The v_2 Landscape: From Hydro to pQCD

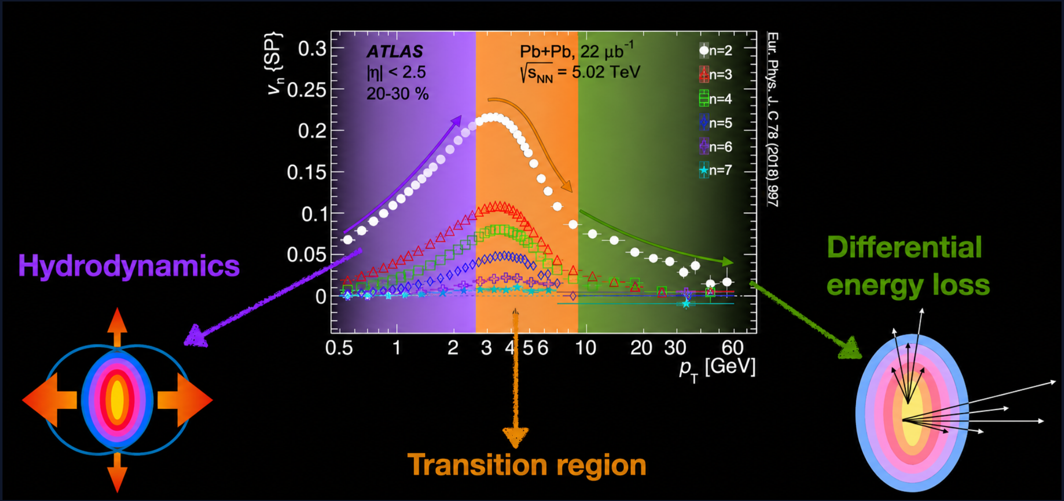

Fig. from Kurt Hill at QM'19

Energy Loss in Small Systems

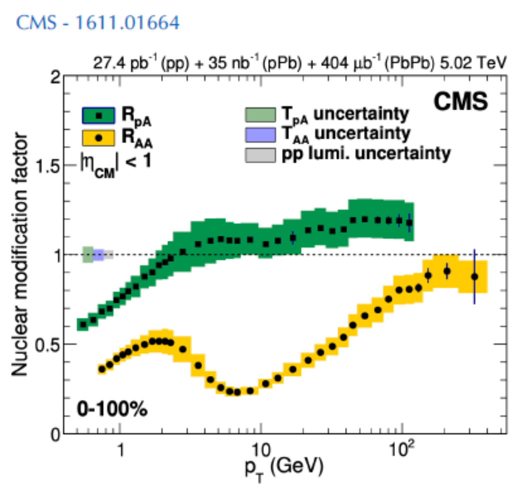

Energy Loss in Small Systems

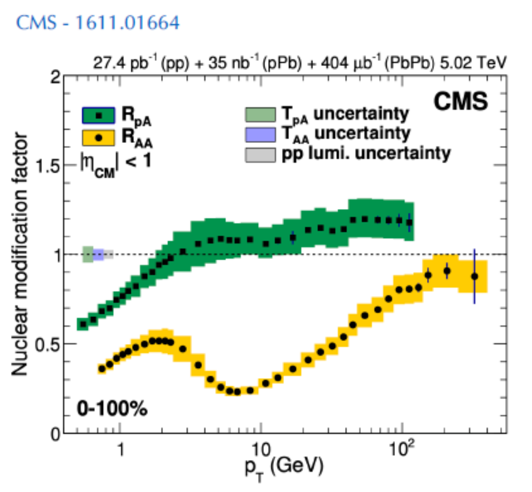

- **The Observation:** No evidence of energy loss in pPb collisions.

Energy Loss in Small Systems

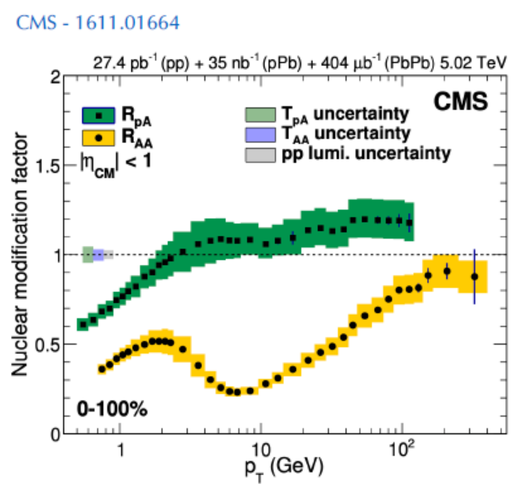

- **The Observation:** No evidence of energy loss in pPb collisions.
- **Hypothesis:** These systems are too small to induce sizeable partonic energy loss.

Energy Loss in Small Systems

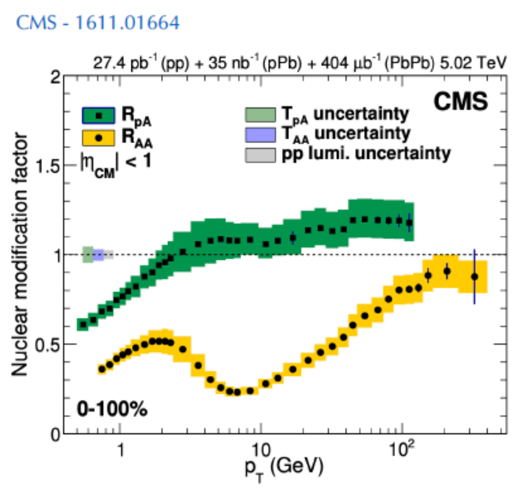

- **The Observation:** No evidence of energy loss in pPb collisions.
- **Hypothesis:** These systems are too small to induce sizeable partonic energy loss.
- **The Puzzle:** Why do then preferred orientations arise at high p_T?

The Puzzle of Small Collision Systems

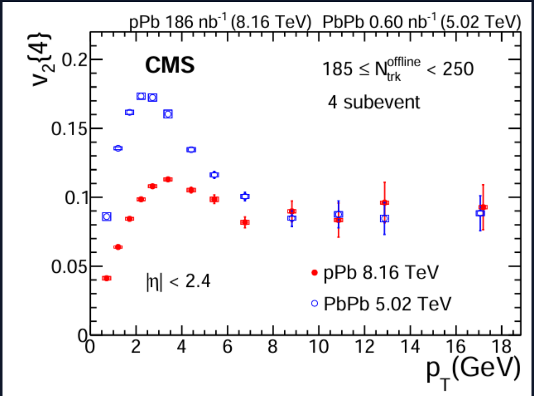

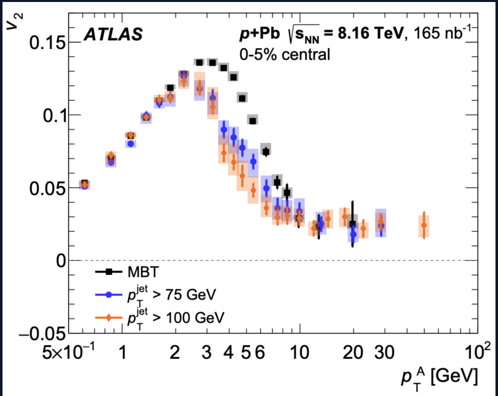

Left: CMS 2502.07525; Right: ATLAS 1910.13978

See also initial state effects from Majumder & Soudi 2308.14702

Our Model

Can we generate preferred orientation without energy loss?

Assume:

- Medium is confined within a region with a boundary.
- Phase shift due to interaction with background field.

$$W[x_f, x_i] = \mathcal{P}e^{ig\int_{x_i}^{x_f} A}$$

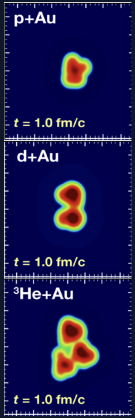

Fig. from PHENIX - Nature Physics 15, 214–220 (2019)

Toy model for a first look

Basic elements:

- Quantum mechanics.

$$(D^2 + m^2)\psi = 0, \;\; D_\mu = \partial_\mu + iqA_\mu.$$

- Constant potential inside a compact region.

$$qA_\mu = (V, 0), \quad \mathcal{W} \sim e^{iVT}$$

Stationary states described by Helmholtz equation:

$$(\nabla^2 + k^2)\psi = 0.$$

- $k_o := \sqrt{E^2 - m^2}$
- $k_i := \sqrt{(E-V)^2 - m^2}$

Boundary integral representation

$$\psi(r) = \int_{\partial\Omega} d\alpha \left(\psi(s)\partial_n G_o(r,s) - G_0(r,s)\partial_n \psi(s)\right)$$

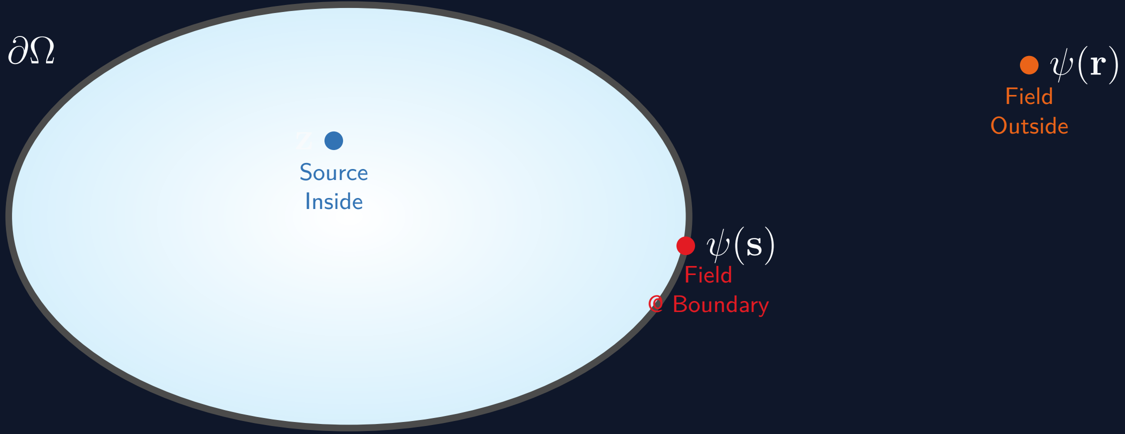

Approximations

- Far-field approximation (detector far away):

$$G_0(s, r) \sim \frac{ie^{ik_o r} e^{-i\pi/4}}{\sqrt{8\pi k_o r}} e^{-ik_o \boldsymbol{s}\boldsymbol{e}}$$

- Plane wave approximation ($k \gg \kappa \sim 1/R$):

$$\psi_i(\boldsymbol{s}, \boldsymbol{z}) \sim \frac{ie^{ik_i|\boldsymbol{s}-\boldsymbol{z}|} e^{-i\frac{\pi}{4}}}{\sqrt{8\pi k_i |\boldsymbol{s} - \boldsymbol{z}|}}$$

Then $\psi(r) = T\psi_i(r)$, $T = (2k_i \cos\theta_i)/(k_i \cos\theta_i + k_o \cos\theta_o)$.

$$\cos\theta_i := \hat{\boldsymbol{u}} \cdot \hat{\boldsymbol{n}} \qquad \hat{u} := \text{incidence angle}$$
$$\cos\theta_o := \hat{\boldsymbol{n}} \cdot \hat{\boldsymbol{e}} \qquad \hat{e} := \text{detector angle}$$

Stationary phase approximation (SPA)

$$\psi(\boldsymbol{r}) \sim \frac{-e^{ik_o r}}{4\pi\sqrt{k_o r}}\sqrt{k_i}\int_{\partial\Omega} d\alpha \frac{\cos\theta_i}{\sqrt{|\boldsymbol{s}-\boldsymbol{z}|}} e^{i\chi(\alpha)}\,,\ \chi(s) \equiv k_i|\boldsymbol{s}-\boldsymbol{z}| - k_o \boldsymbol{s}\cdot\hat{\boldsymbol{e}}$$

Rapid oscillating phase allows us to use the SPA:

- First derivative (Snell's law)

$$\chi'(\alpha)\Big|_{\alpha=\alpha^*} = 0 \rightarrow k_i \hat{\boldsymbol{u}}\cdot\hat{\boldsymbol{t}} = k_o \hat{\boldsymbol{e}}\cdot\hat{\boldsymbol{t}}.$$

- Second derivative

$$\chi''(\alpha) = \frac{k_i\cos^2\theta_i}{|\boldsymbol{s}-\boldsymbol{z}|} + \kappa(k_o\cos\theta_o - k_i\cos\theta_i).$$

- Amplitude:

$$\mathcal{A}^S(\phi) \sim \frac{k_i\cos^2\theta_i}{|k_i\cos^2\theta_i + L\kappa(k_o\cos\theta_o - k_i\cos\theta_i)|}$$

An Estimate for v_2

$$v_2 \approx \frac{1}{2} \frac{\mathcal{A}_{\text{short}} - \mathcal{A}_{\text{long}}}{\mathcal{A}_{\text{short}} + \mathcal{A}_{\text{long}}} = \frac{V(2-e^2)e^2}{4(1-e^2)k_o + 2e^4 V}$$

An Estimate for v_2

$$v_2 \approx \frac{1}{2}\frac{\mathcal{A}_{\text{short}} - \mathcal{A}_{\text{long}}}{\mathcal{A}_{\text{short}} + \mathcal{A}_{\text{long}}} = \frac{V(2-e^2)e^2}{4(1-e^2)k_o + 2e^4 V}$$

- Vanishes when $e = 0$ (circle).

An Estimate for v_2

$$v_2 \approx \frac{1}{2}\frac{\mathcal{A}_{\text{short}} - \mathcal{A}_{\text{long}}}{\mathcal{A}_{\text{short}} + \mathcal{A}_{\text{long}}} = \frac{V(2-e^2)e^2}{4(1-e^2)k_o + 2e^4 V}$$

- Vanishes when $e = 0$ (circle).
- Vanishes when $V = 0$.

An Estimate for v_2

$$v_2 \approx \frac{1}{2}\frac{\mathcal{A}_{\text{short}} - \mathcal{A}_{\text{long}}}{\mathcal{A}_{\text{short}} + \mathcal{A}_{\text{long}}} = \frac{V(2-e^2)e^2}{4(1-e^2)k_o + 2e^4 V}$$

- Vanishes when $e = 0$ (circle).
- Vanishes when $V = 0$.
- Is positive, grows with e and V.

An Estimate for v_2

$$v_2 \approx \frac{1}{2} \frac{\mathcal{A}_{\text{short}} - \mathcal{A}_{\text{long}}}{\mathcal{A}_{\text{short}} + \mathcal{A}_{\text{long}}} = \frac{V(2-e^2)e^2}{4(1-e^2)k_o + 2e^4 V}$$

- Vanishes when $e = 0$ (circle).
- Vanishes when $V = 0$.
- Is positive, grows with e and V.
- Scales like $\sim 1/k$.

An Estimate for v_2

$$v_2 \approx \frac{1}{2}\frac{\mathcal{A}_{\text{short}} - \mathcal{A}_{\text{long}}}{\mathcal{A}_{\text{short}} + \mathcal{A}_{\text{long}}} = \frac{V(2-e^2)e^2}{4(1-e^2)k_o + 2e^4 V}$$

- Vanishes when $e = 0$ (circle).
- Vanishes when $V = 0$.
- Is positive, grows with e and V.
- Scales like $\sim 1/k$.
- Does not depend on the system size.

Constructive and destructive interference

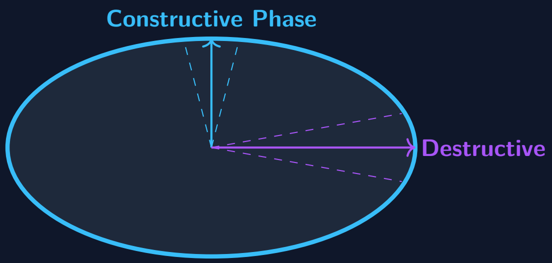

- More similar nearby paths interfere less destructively.

Constructive and destructive interference

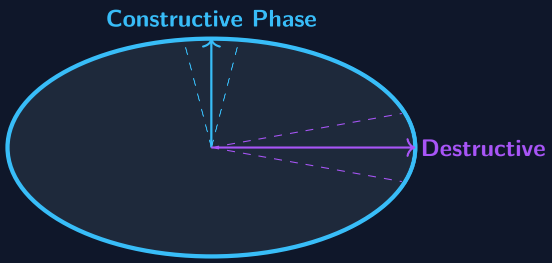

- More similar nearby paths interfere less destructively.
- There is a preference for low curvature exit points.

Constructive and destructive interference

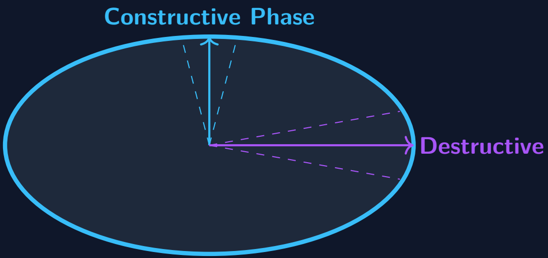

- More similar nearby paths interfere less destructively.
- There is a preference for low curvature exit points.
- The amount of paths scales with wavelength.

Constructive and destructive interference

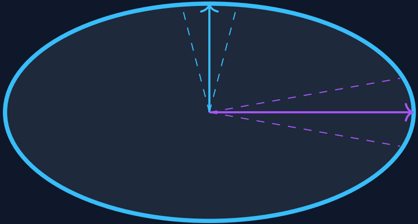

- More similar nearby paths interfere less destructively.
- There is a preference for low curvature exit points.
- The amount of paths scales with wavelength.
- The effect fades away when the boundary is perceived as flat.

Exact Solution for Elliptic Medium

Solving the Helmholtz equation in elliptic coordinates

$$x = \cosh\mu \cos\nu$$
$$y = \sinh\mu \sin\nu$$

enables to

$$\psi(\mu, \nu) = M(\mu) N(\nu),$$

and

$$\frac{d^2 N}{d\nu^2} + (\lambda_q - 2q\cos 2\nu) N = 0\,,$$
$$\frac{d^2 M}{d\mu^2} - (\lambda_q - 2q\cosh 2\mu) M = 0.$$

$q = \frac{c^2 k^2}{4}$

Matching at the Boundary

We can expand the solution inside and outside of the medium:

$$\psi_s = \sum_{m=0}^{\infty} \alpha_m \, \mathrm{ce}_m(\nu, q_i) \, \mathrm{Mc}_m^{(3)}(\mu, q_i) + (\text{odd}) \,,$$

$$\psi_r = \sum_{m=0}^{\infty} A_m \, \mathrm{ce}_m(\nu, q_i) \, \mathrm{Mc}_m^{(1)}(\mu, q_i) + (\text{odd}) \,,$$

$$\psi_i = \psi_s + \psi_r .$$

$$\psi_o(\mu, \nu) = \sum_{m=0}^{\infty} C_m \, \mathrm{ce}_m(\nu, q_o) \, \mathrm{Mc}_m^{(3)}(\mu, q_o) + (\text{odd})$$

Imposing boundary conditions (μ_0 the limit of the region):

$$\begin{aligned} \psi_i(\mu_0, \nu) &= \psi_o(\mu_0, \nu) \\ \partial_\mu \psi_i(\mu_0, \nu) &= \partial_\mu \psi_o(\mu_0, \nu) \end{aligned}$$

It allows us to solve for C_m, which are the transmission coefficients.

We have a mix of modes:

$$\mathrm{O}_{nm}(q_i, q_o) = \int_0^{2\pi} \mathrm{ce}_m(\nu, q_i) ce_n(\nu, q_o) \neq \delta_{nm}$$

Results

- Compute v_2 as

$$v_2 = \frac{\displaystyle\int_0^{2\pi} \cos(2(\phi - \Psi_2))\mathcal{A}(\phi)d\phi}{\displaystyle\int_0^{2\pi} \mathcal{A}(\phi)d\phi}$$

  where $\mathcal{A}(\phi) \sim |\psi_o|^2$ at $\mu \to \infty$ is amplitude at detector.

- Present v_2 as a function of:
  - System size R.
  - Centrality (maps to eccentricity e).
  - Detected particle energy k_o.

Results

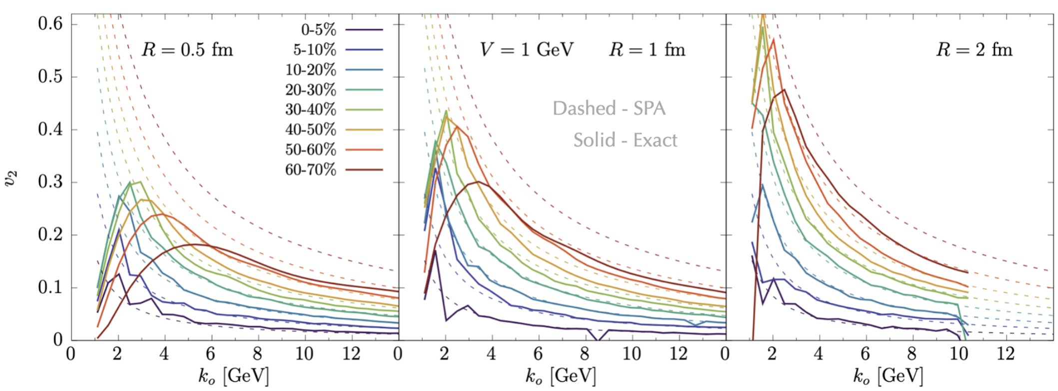

0.6
0.5
0.4
0.3
0.2
0.1
0
v_2
$R = 0.5$ fm
0-5%
5-10%
10-20%
20-30%
30-40%
40-50%
50-60%
60-70%
$V = 1$ GeV
$R = 1$ fm
Dashed - SPA
Solid - Exact
$R = 2$ fm
0 2 4 6 8 10 12
k_o [GeV]

Transmitted Norm

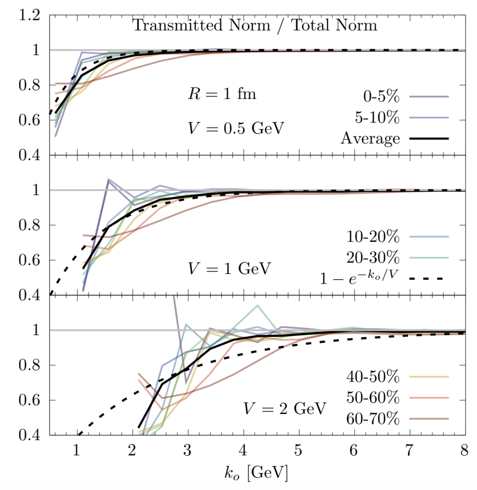

$$R := \frac{\oint A(V \neq 0)}{\oint A(V = 0)}$$

- Norm quickly approaches one already at fairly low k_o.
- Averaged reflected norm roughly follows $e^{-k_o/V}$.
- No spectrum shift (no "energy loss"), and still large v_2.

So far

- Toy model with constant electrostatic potential
- Standard quantum mechanics

Let us move towards a more realistic scenario.

Jet Quenching Formalism

- Let's consider a hard colored parton traveling through a medium:

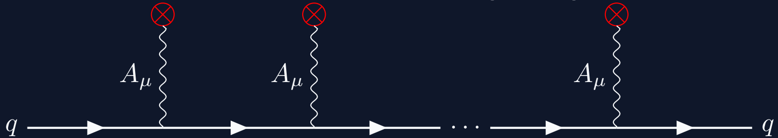

- In light-cone coordinates, the retarded propagator solves the Schrödinger equation

$$i\partial_z \mathcal{G}_R(z,\boldsymbol{x};z_i,\boldsymbol{x}_i) = \left[-\frac{\nabla^2_{\boldsymbol{x}}}{2E} + gA^-_a(z,\boldsymbol{x})T^a_R\right]\mathcal{G}_R(z,\boldsymbol{x};z_i,\boldsymbol{x}_i),$$

Can we account for the non-trivial support of the deconfined medium?

Boundary Integral Representation

$$\mathcal{G}_R(X;X_i) = i\int_\Sigma d\Sigma_\mu(S)\, J^\mu[\mathcal{G}_0(X;S),\mathcal{G}_R(S;X_i)]\,, \qquad J^\mu[g,h] = \left(igh,\ \frac{1}{2E}\, g \overleftrightarrow{\nabla}_{\boldsymbol{y}} h\right)$$

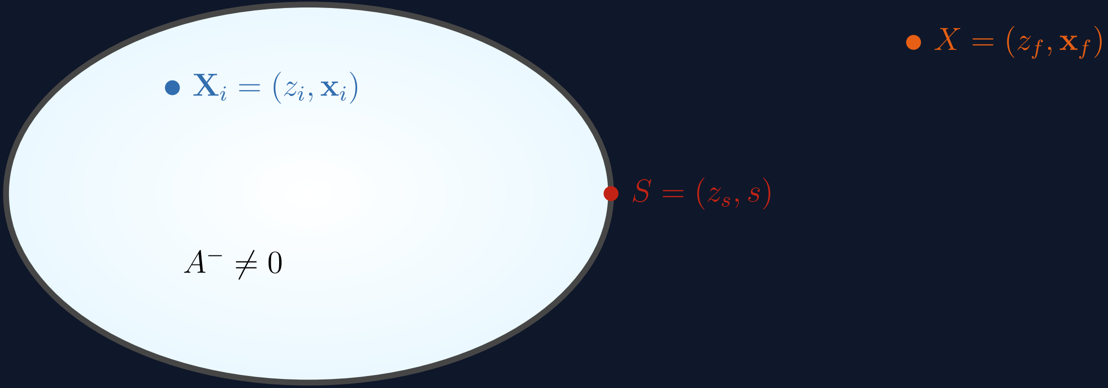

Amplitude

The exact amplitude can be computed as

$$\frac{dN}{dEdp} = \langle \mathcal{A}_R(p)\mathcal{A}_R^*(p)\rangle = \frac{1}{2\pi}\int_\Sigma dsd\bar{s}e^{-ip(s-\bar{s})+i\frac{p^2}{2E}(z_s-z_{\bar{s}})}\langle \mathcal{Q}_R(S)\mathcal{Q}_R^\dagger(\bar{S})\rangle\,,$$

where we have defined

$$\mathcal{Q}_R(S) = \psi_R(S) + \frac{iz_s'}{2E}\left(\partial_s\psi_R(S) + ip\,\psi_R(S)\right)$$

and

$$\psi_R(S) = \int dx_i\,\mathcal{G}_R(S;X_i)\left(\frac{w^2}{\pi}\right)^{1/4}\exp\left[-\frac{w^2(x_i-x_0)^2}{2}\right]\,,$$

where $\delta \equiv \frac{1}{w}$ is the transverse extent of the initial wave packet.

Eikonal Limit

- If we take $E \to \infty$

$$\mathcal{G}_R \to \mathcal{G}_0\, U_R$$

- The amplitude is simplified

$$\frac{dN}{dEdp} = \langle \mathcal{A}_R(p)\mathcal{A}_R^*(p)\rangle = \frac{1}{2\pi}\int_\Sigma ds d\bar{s} e^{-ip(s-\bar{s})+i\frac{p^2}{2E}(z_s - z_{\bar{s}})}\mathcal{W}_R\,,$$

- One obtains the dipole correlator

$$\mathcal{W}_R(S;\bar{S}) = \frac{1}{d_R}\langle \mathrm{Tr}_R\, U(z_s, s)U(z_{\bar{s}}, \bar{s})\rangle$$

Homogeneous Stochastic Medium

- Let's consider a homogeneous thermal stochastic 2D medium with a *sharp boundary*:

$$\left\langle A_a^-(\xi,x)A_b^-(\eta,y)\right\rangle = \Theta_\Omega(\xi,x)\Theta_\Omega(\eta,y)\delta_{ab}\,\delta(\xi-\eta)\int\frac{dq}{2\pi}\,n_0\,\frac{g^4}{(q^2+\mu^2)^2}\,e^{iq(x-y)}$$

- The dipole can be obtained analytically as $\mathcal{W}_R(S;\bar{S}) = \exp(-D(z_s,s;z_{\bar{s}},\bar{s}))$,

$$\mathcal{D}(z_s,s;z_{\bar{s}},\bar{s}) = \frac{C_R}{2}\int_0^\infty d\xi\int\frac{dq}{2\pi}\,\mathcal{C}(q)\left[\Theta_s(\xi)+\Theta_{\bar{s}}(\xi)-2\Theta_s(\xi)\Theta_{\bar{s}}(\xi)\cos\left(qr(\xi)\right)\right]$$

- Computing the integral

$$\mathcal{D}(z_s,s;z_{\bar{s}},\bar{s}) = \frac{C_R n_0 g^4}{8\mu^3}\left(z_s+z_{\bar{s}}-2z_<(1+\mu|s-\bar{s}|)e^{-\mu|s-\bar{s}|}\right).$$

Computing v_n

- Which is the probability that a particle with large energy E in direction ϕ_i ends up at detector angle ϕ?

$$\mathcal{Y}(\phi) = \int \frac{d\phi_i}{2\pi} \int_{-p_c}^{p_c} dp\, \mathcal{I}(p, \phi_i) \delta(\phi_i + \frac{p}{E} - \phi).$$

- Then, we can compute

$$v_n \equiv \frac{\int d\phi \mathcal{Y}(\phi) \cos(n(\phi - \Psi_n))}{\int d\phi \mathcal{Y}(\phi)}.$$

- Useful to have an analytic approximation for v_n. Let's define $\Delta = s - \bar{s}$ and $\alpha_R = \frac{C_R n_0 g^4}{\mu^3} = \hat{q}/\mu^2$.

Central Ray Limit $\Delta \to 0$

In the central-ray approximation (appropriate for high E), we define

$$z(\phi) \equiv z_\phi(0), \qquad z'(\phi) \equiv \left.\frac{\partial z_\phi(s)}{\partial s}\right|_{s=0}.$$

For a hard boundary with support imposed directly on the field correlator, the small-separation dipole exponent is

$$D(\phi,\Delta) \simeq \frac{\alpha_R}{2}|z'(\phi)|\,|\Delta| + \frac{\alpha_R}{2} z(\phi)\mu^2\Delta^2 + \cdots .$$

The momentum-broadening kernel at fixed incoming angle is then

$$\mathcal{I}(p,\phi) = \frac{1}{\pi}\int_0^\infty d\Delta\,\cos(p\Delta)\,\exp\left[-\frac{w^2\Delta^2}{4} - \frac{\alpha_R}{2}|z'(\phi)|\Delta - \frac{\alpha_R}{2}z(\phi)\mu^2\Delta^2\right].$$

v_2 from Central Ray Limit

- For $n = 2$ and short-axis event plane $\Psi_2 = \pi/2$,

$$v_2 = -e^{-w^2/E^2} \int_0^{2\pi} \frac{d\phi}{2\pi} \cos(2\phi) \exp\left[-\frac{\alpha_R}{E}|z'(\phi)| - \frac{2\alpha_R \mu^2}{E^2} z(\phi)\right].$$

We get an intensive (curvature-dependent) and an extensive (size-dependent) contribution.

- For the case of an ellipse

$$v_2 = -e^{-w^2/E^2} \frac{2}{\pi} \int_0^{\pi/2} d\phi \cos(2\phi) \exp\left[-\frac{\hat{q}}{\mu^2 E}\left(\frac{e^2 \sin\phi \cos\phi}{1 - e^2 \cos^2\phi} + \frac{2\mu^2}{E} \frac{b}{\sqrt{1 - e^2 \cos^2\phi}}\right)\right].$$

b is minor semi-axis.

Results: Check of Central Ray Limit

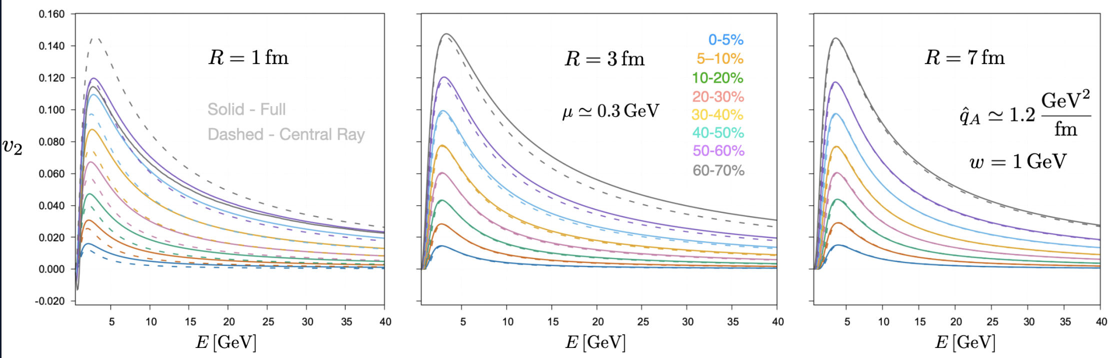

Results: Dependence on Debye Mass μ

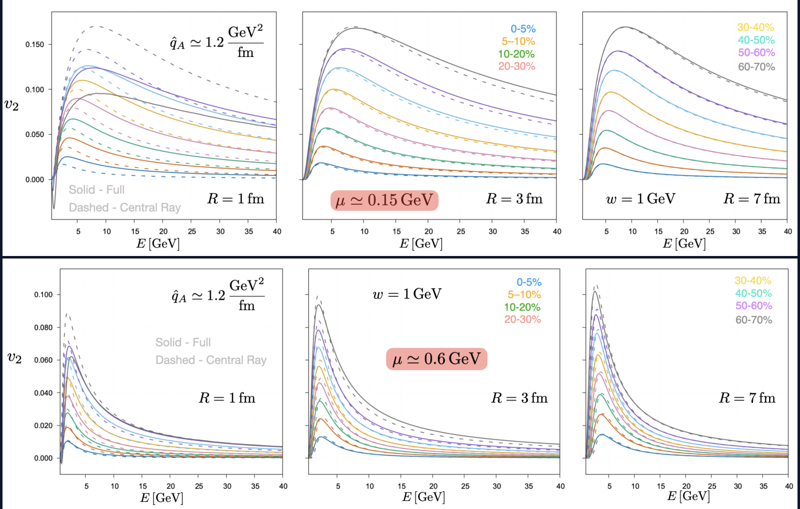

Results: Intensive vs Extensive in Central Ray Limit

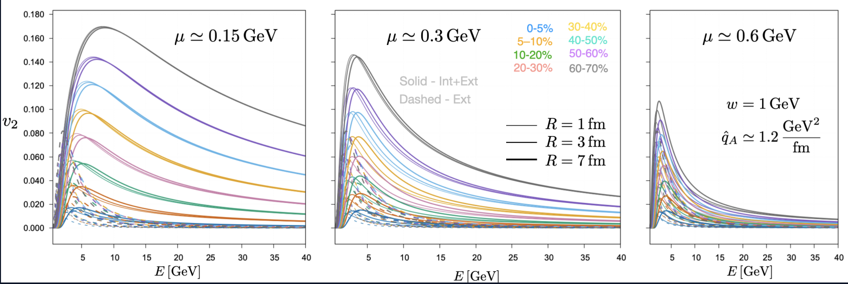

Transverse color decoherence (extensive) contributes at smaller λ and dominates at larger μ.

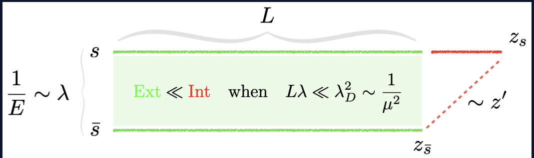

$l_F \equiv \sqrt{\lambda L}$ is Fresnel scale in optics.
λ_D acts as an aperture.
$l_F \ll \lambda_D$ would be near-field regime.

Conclusions

New mechanism to produce azimuthal anisotropies based on the interplay of

- Deconfined **medium geometry**.
- In-medium quantum **phase shifts**.

Explored different scenarios with similar qualitative results:

- **Toy model:** Constant electrostatic potential in QM.
- **Jet quenching formalism**: Stochastic, locally homogeneous medium in QFT.
  - Color decoherence modifies angular distribution depending on explored geometry.

Working towards a more realistic phenomenology. So far:

- System size independence at high E, driven by curvature effects.
- Non-monotonic behaviour at smaller E, driven by finite system size effects.

Outlook: Full Sub-Eikonal Results

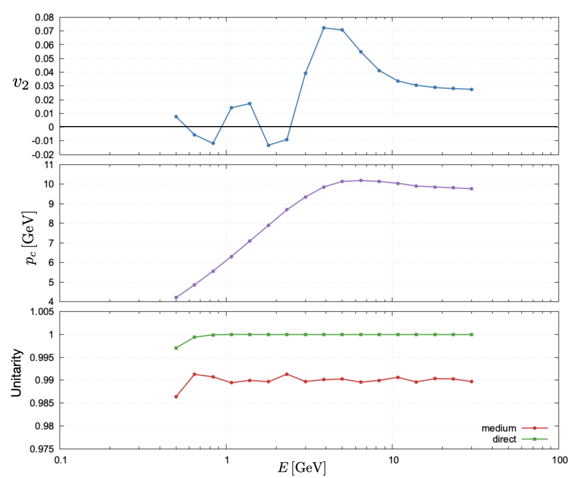

For small E we need to compute sub-eikonal effects coming from flux factors (J^μ) and broadening (∇_x^2).

Started using the usual harmonic oscillator approximation.

Outlook: Smeared Potential

Consider long-tailed fields generated by scattering centres within an ellipse:

$$A_a^-(\xi, x) = \int du\, \mathcal{G}_\mu(x-u)\, \rho_a(\xi, u), \qquad \mathcal{G}_\mu(x) = \frac{g^2}{2\mu} e^{-\mu|x|}.$$

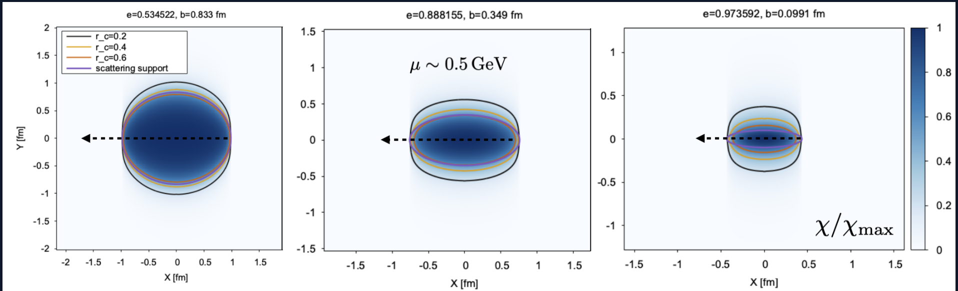

χ is the local field-correlator squared potential. Long tails deform boundary geometry, specially if $\lambda_D \sim L$. *What would be a better description of the background field within deconfined media?*

Outlook: Smeared Potential

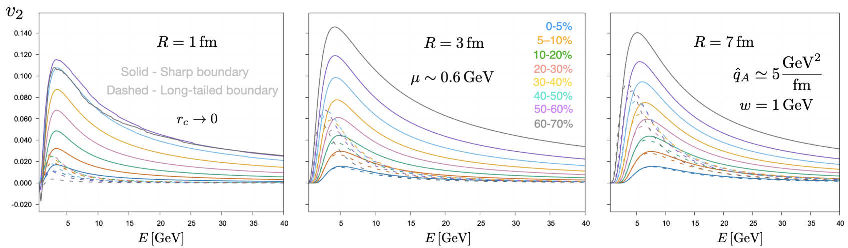

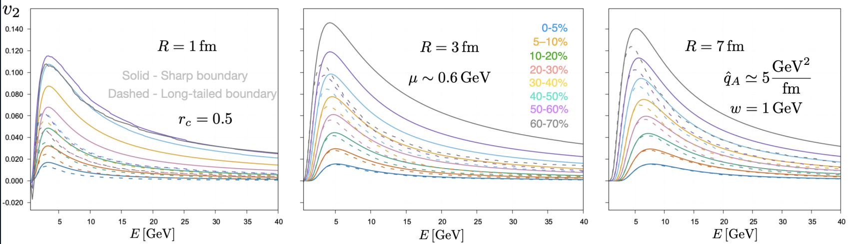

Thank you for your attention!